Journal of Physics: Conference Series **335** (2011) 012071 doi:10.1088/1742-6596/335/1/012071

The NA62 experiment at CERN

Gianluca Lamanna

CERN, CH-1211 Geneve 23, Switzerland

E-mail: gianluca.lamanna@cern.ch

Abstract. The Branching Ratio (BR) of the rare decay $K^+ \to \pi^+\nu\bar{\nu}$ is predicted with a small error in the framework of the standard model (SM). The contribution of long distance terms is suppressed thanks to the GIM mechanism and the short distance dynamics is almost completely described by well measured semileptonic operators. The cleanness of the SM prediction together with the small BR ($\sim 10^{-10}$) makes this decay an interesting opportunity to describe the presence and the contribution of the new physics using relatively low energy processes. The NA62 experiment at CERN aims at measuring O(100) events in two years of data taking with 10% background. From an experimental point of view this measurement is very challenging because the weakness of the signal signature and the huge amount of background processes. In this paper the key points of the experiment will be described after a brief introduction on theoretical aspects and present results.

1. Introduction

Among the GIM suppressed rare decays in B and K meson, the $K \to \pi\nu\bar{\nu}$ processes play an important role in search for new physics. These decays are completely dominated by short distance dynamics and the amplitude is governed by just one single semileptonic operator, defined using the well measured semileptonic kaon decays. The relevant diagrams are boxes and penguins where the top contribution is dominant. The contribution from the CKM dynamics comes from the top coupling with d and s quark. For that reason the matrix element is proportional to λ^5 and the BR is very small. For what concerns the $K^+ \to \pi^+\nu\bar{\nu}$ a small contribution from the c quark coupling has to be taken into account. This contribution gives an irreducible theoretical error of 3% in the BR prediction, while all the other contributions in the total error are parametric, depending on measured quantities. The present SM prediction [1], including NNLO QCD corrections [2], electroweak corrections [3] and long distance contribution [4] is

$$BR(K^+ \to \pi^+\nu\bar{\nu}) = (8.5 \pm 0.7) \cdot 10^{-11}$$

The $K_L \to \pi^0\nu\bar{\nu}$ is also cleaner from a theoretical point of view, with an irreducible error of $\sim 1\%$. The precision in the prediction for these decays allows a stringent test for the SM and, at the same time, a very powerful research for new physics beyond the SM. Several extensions, including models with 4^{th} quarks generation [5], Littlest Higgs [6], Randall and Sundrum mechanism [7] and supersymmetric flavour models [8], give sizable differences in both $K^+ \to \pi^+\nu\bar{\nu}$ and $K_L \to \pi^0\nu\bar{\nu}$ branching ratios. For that reason the measurement of these decays will be very important not only to understand the magnitude of contribution of new physics, but also to distinguish among different models. Nevertheless the very good precision in theoretical prediction needs an experimental measurement with compatible error. At the

Published under licence by IOP Publishing Ltd

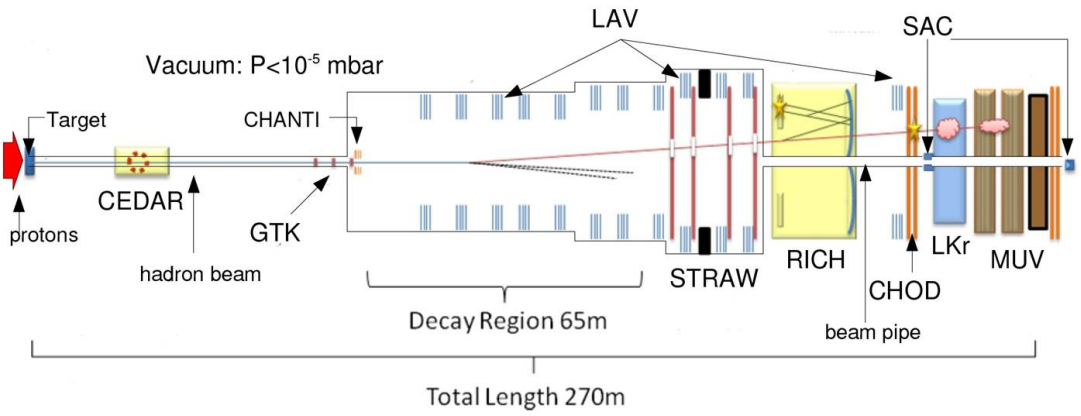

Figure 1. NA62 experiment layout.

moment the experimental precision is quite far from the goal. In particular in the $K^+ \to \pi^+\nu\bar{\nu}$ the most precise results have being obtained by the E787 and E949 experiments at BNL, by studying stopped kaon [9]. The final BR result

$$BR(K^+ \to \pi^+\nu\bar{\nu}) = (17.3^{+11.5}_{-10.5}) \cdot 10^{-11}$$

is based on 7 measured events.

The NA62 experiment aims at measuring O(100) events in about 2 years of data taking, with a small systematic uncertainty. To this purpose at least 10^{13} K^+ decays are required, assuming an acceptance of 10%. To obtain a contribution of the background below 10% a factor of 10^{12} in rejection the other kaon decay mode is needed. Signal acceptance, high intensity beam and rejection factor for the background drive the NA62 design, as will be described in the following.

2. NA62: general overview

In figure 1 the experimental layout is shown. The hadronic beam, composed by $\sim 6\%$ of kaons, is produced by using the 400 GeV/c proton beams coming from the SPS accelerator, impinging in a 40 cm long beryllium target. The beam transport system allow to select an unseparated hadron beam with a momentum of 75 GeV/c and spread of 1%. Differently with respect to the previous experiments, the NA62 technique is based on such high energy beam, instead of using stopped kaons. The advantage of this is both in the possibility to have an intense secondary beam and a higher energy in the decay products of the kaons: thanks to that the requirements to the photon veto system, a very essential part of the experiment as we will see, can be easily fulfilled. On the other hand the use of a high energy hadron beam imply a long decay region and the impossibility to separate the secondary beam components. In any case the large fraction of the decay products of pions present in the beam remains along the beam trajectory, thanks to the large longitudinal momentum with respect the transverse momentum of the decay. Nevertheless the kaon is positively identified in the beam. The decay region begins ~ 100 m after the target, and is housed in a ~ 117 m long and 2.4 m diameter (in average) vacuum tube. The vacuum inside the decay region is maintained at the level of 10^{-6} mbar using diffusion cryogenic pumps, in order to reduce the secondary interaction of the K decay products and to avoid, as much as possible, inelastic scattering of the pions present in the beam. Along the decay region a system is placed in order to veto events not fully contained in the acceptance of the downstream detectors. The momentum of the K decay products is measured inside the vacuum by a spectrometer based on straws chambers and other detectors, described in details in the following, are employed for particle identification and vetoing. The detector

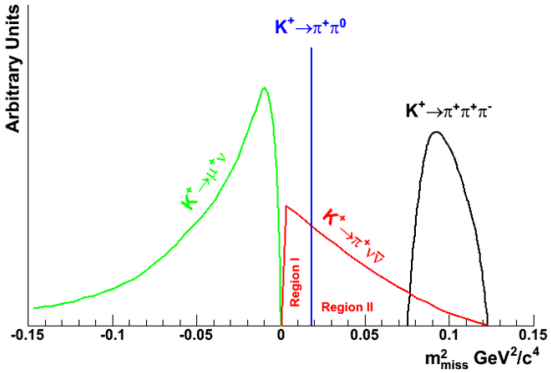

Figure 2. Distribution of kinematically constrained background.

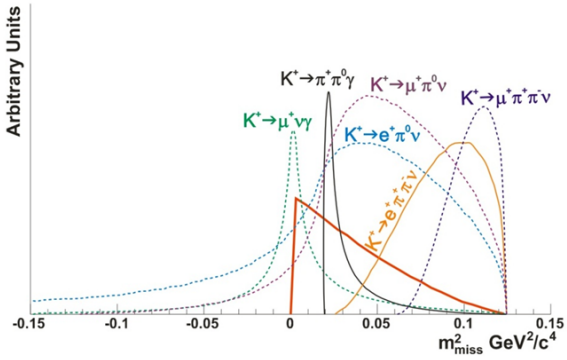

Figure 3. Distribution of not kinematically constrained background.

is designed to have a complete coverage for the K decay products: the very feeble branching ratio and the weak experimental signature, impose an identification of the decay channel on event-by-event base. In table 1 the main K decay modes are listed. The $\pi^+\pi^0$ and the $\mu\nu$ are

Table 1. Branching ratio of the main K decay modes.

Decay mode	Branching Ratio
$\mu^+\nu$	63.5%
$\pi^+\pi^0$	20.7%
$\pi^+\pi^+\pi-$	5.6%
$e^+\pi^0\nu$	5.1%
$\mu^+\pi^0\nu$	3.3%
$\pi^+\pi^0\pi^0$	1.8%

clearly the most dangerous, but almost any decay mode could be a sources of background. In order to reduce the contribution of the spurious decay modes, the background is studied as a function of the squared missing mass, defined below . In the Fig.2 is shown that two regions with potentially good signal to noise ratio can be identified in the "ideal" missing mass distribution. In the real world a good kinematic reconstruction has to be applied in order to have negligible contribution of resolution tails in the signal regions. We refer to the background that can be separated using the signal regions definition as "kinematically constrained". This amounts to $\sim$ 92% of the total background. The remaining $\sim$ 8% is "not kinematically constrained" and spans over the whole range of the missing mass distribution, as shown in Fig.3. The rejection of this component of the background is completely based on the efficiency of particle rejection and identification. The tolerable level of background is around 10% of the signal events. In order to collect O(100) events in a reasonable data taking period, the intense kaon beam produces about 10 MHz of events in the downstream detectors. Particular care has been devoted in designing an efficient data acquisition and trigger system to cope with a big data flux without introducing any kind of additional inefficiency. Summarizing, the key components of the experiment are: a

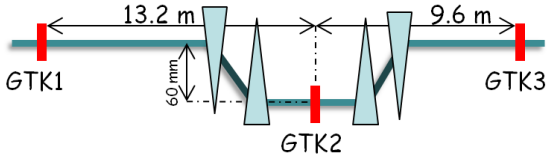

Figure 4. The GTK momentum measurement principle.

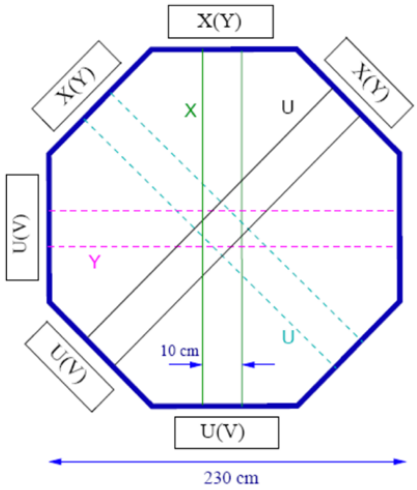

Figure 5. Straws disposition in a chamber.

good kinematic rejection in order to reduce the kinematically constrained background, a high efficiency veto system and particle identification to recognize the not kinematically constrained kaon decays and the resolution tails of the main decay modes, and a trigger system to allow a reliable, lossless and efficient data acquisition at high rate. In the next sections these points will be presented in details.

3. Kinematics rejection

The signal region, as already mentioned above, is defined using the kinematics of $K^+ \to \pi^+\nu\bar{\nu}$. In particular the squared missing mass (m^2_{miss}) defined as the squared difference of K^+ and downstream single track in the π^+ hypothesis 4-momenta. This variable separates the signal from most of the kaon decays, as already shown in Fig.2. Although clean regions can be defined exploiting the kinematic reconstruction of the background events (mainly $\pi^+\pi^0$ and $\mu^+\nu$), resolution effects can bring non-signal events in the signal regions. To increase the resolution in the m^2_{miss} variable, both kaon and pion momenta have to be measured with high precision and with small non-gaussian tails. For that reasons the multiple scattering has to be reduced as much as possible by using light mass detectors placed in vacuum. In addition, the beam spectrometer (for the kaons) and the downstream spectrometer (for the pions) information has to be associated with a good time resolution, due to the high intensity beam.

The designed beam spectrometer, called GigaTracker (GTK), consists of 3 Silicon pixel stations. Each station is 6.3x2.9 cm^2 to match the beam dimension. A system of analyzing dipole magnets, as shown in figure 4, allow to measure momentum and direction of any particle in the beam (about 800 MHz). The detector has to be very thin in order to reduce the multiple scattering: 200 μm for the Si sensor and 100 μm for the bump bonded readout chip. The achievable time resolution has been measured at a test beam to be better than 200ps. The whole detector will count about 18000 pixels, with a maximum rate of 150 kHz per pixel in the central part. Particular care has been devoted to the cooling system design in order to decrease the contribution of the leakage current in a radiation hard environment. The resolution in the momentum measurement will be in the order of $\sim 0.2\%$ for 75 GeV/c particles, while the direction will be measured with a precision of ~ 16 μrad.

The downstream spectrometer is formed by four chambers made with 9.6 mm in diameter

straw tubes and one dipole magnet. To reduce the multiple scattering the spectrometer is placed in the same decay region vacuum. Each chamber is equipped with 16 planes of 2.1 m long tubes oriented in the x, y and ±45 degrees directions. In each plane a strip in the central part is keept free from tubes in order to create an octagonal hole around the center of the chamber where the beam of undecayed particles passes through (see figure 5). The resolution of this system is (in GeV/c):

$$\frac{\sigma(P_\pi)}{P_\pi} = 0.3\% \oplus 0.007\% \cdot P_\pi$$

$$\frac{\sigma(dX/dZ)}{dX/dz} = 15 - 45\mu rad$$

The STRAWS and the GigaTracker allow to have a 10^4 and 10^5 rejection factor on $K^+ \to \pi^+\pi^0$ and $K^+ \to \mu^+\nu$, with a definition of the signal region sufficient to have 10% acceptance.

4. Veto system

The kinematic constrains are not enough to reject all the $K^+ \to \pi^+\pi^0$ and $K^+ \to \mu^+\nu$. The additional rejection factor, independent from the kinematics, will be given by the direct detection of γ and μ. Moreover the detection of the not constrained background is completely based on the particle detection. The muon detection will be discussed in the next session. The photon veto system design is driven by the necessity to detect the $K^+ \to \pi^+\pi^0$ with an inefficiency at the level of 10^{-8} for the π^0. In order to cover the whole acceptance for the γ's, the veto system is subdivided into different detector: the large angle veto (LAV) in the region between 8.5 and 50 mrad, the LKr calorimeter in forward region between 1 and 8.5 mrad, and the small angle vetoes (SAV), for gammas with angle less than 1 mrad.

The requirement for the LAV is to have an inefficiency on single photon detection at level of 10^{-4}, in the energy range from 200 MeV up to several tens of GeV. The LAV is made of 12 stations placed along the decay region, inside the spectrometer and after the RICH; three possible options have been tested: scintillating fibers and lead (KLOE calorimeter like), scintillator and lead tiles or lead-glass crystals (from the OPAL calorimeter). Details of the prototypes studies could be found in [10]. All the options match the requirement of 10^{-4} inefficiency, the lead glass solution has been selected. In each station the lead glass blocks are disposed radially in five rings in order to assure at least $20X_0$ (three blocks) hit by any gamma impinging on the detector (figure 6). The whole system uses more than 2500 lead glass crystals. The time resolution has been measured at a test beam to be better than 700 ps.

For the forward gammas the requirements in terms of photon veto inefficiency depend on the energy, going from 10^{-3} for 1 GeV up to 10^{-6} for energy greater than 10 GeV. The LKr calorimeter is a quasi-homogeneous electromagnetic calorimeter $27X_0$ in depth, with a good energy, position and time resolutions, built for the NA48 experiment [11]. It's composed by more than 13000 $2 \times 2cm^2$ cells, continuously digitized at 40 MHz. The performance as photon veto detector has been measured in a special run in 2006 on a 75 GeV/c kaon beam. The readout electronics will be completely rebuilt in order to cope with the higher rate with respect to the NA48 runs.

The region below 1 mrad is covered by two detectors: the IRC and the SAC. Both are Shashlyk calorimeter. The first is placed in front of the LKr to cover the region around the beam pipe where the calorimeter is not efficient enough, the second is placed at the very end of the experiment, in the beam dump, to catch the gammas from the π^0 remaining inside the beam pipe. The undecayed charged beam is deflected before this detector. Before the decay region, an additional charged particles veto, the CHANTI, is placed around the third GTK station to detect the hadronic interactions in the beam spectrometer.

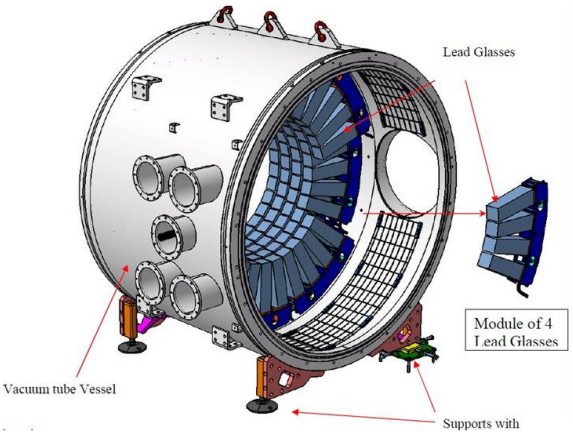

Figure 6. Lead-glass blocks in a LAV station.

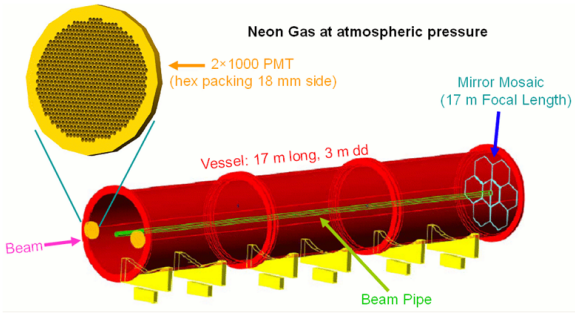

Figure 7. The RICH detector.

5. Particle identification

Mainly to reject the dominant $K^+ \to \mu^+\nu$, decay a redundant particle identification system has been designed, to provide the additional 10^4 rejection factor. The PID system is also employed (in some case together with the veto system) to reach the rejection power for not constrained decay with muons or electrons (as, for instance, $K^+ \to \mu^+\pi^0\nu$ and $K^+ \to e^+\pi^0\nu$).

The RICH (figure 7) is built in a 17 m long and 2 m in diameter vessel, with 1 atm Neon as radiator. The Cherenkov light is focused by two mirrors of 17 m of focal length in two spots covered by about 1000 phototubes each. The phototubes are 1.8 cm in diameter with a quantum efficiency sufficient to have about 18 photo-electrons per rings generated by 35 GeV/c pions. The separation inefficiency between pion and muon is below 1% in the range 15-35 GeV/c . The very good time resolution of 70 ps per track is exploited to match the decay information with the kaon passed inside the GTK.

The MUV, placed after the LKr calorimeter, is subdivided in three subsystems: the MUV1 and MUV2 are composed by iron and scintillators to measure the shape and the energy deposition of the impinging particle to distinguish between muons and pions. The MUV3, placed after a further 80 cm iron wall, is used as fast muon detector for trigger purposes.

For what concerns the electrons identification the RICH and LKr, comparing the electromagnetic energy and the momentum measured by the STRAWS, will be used.

The CEDAR is a differential Cherenkov detector made with H_2 at 1 atm and placed before the GTK, directly on the unseparated hadron beam. Through an optical system made with mirrors and slits, the Cherenkov ring, coming from kaons, is observed in 8 spots, using photomultipliers. In order to decrease the rate per phototubes, the Cherenkov light in each spot is spread in a large surface covered by several phototubes. The main purpose of this detector is to positive identify the kaon to reduce the contribution of the pion from the beam scattering on the residual gas in the decay region.

6. Trigger system

The rate of events in the decay region is strongly dominated by background. According to preliminary simulations the rate on the main detectors is around 10 MHz (table 2). An additional rate of at least ~ 1 MHz of muons coming from the beam production target, must be taken into account. In this environment the requests to the DAQ and trigger systems are:

- Very low DAQ inefficiency ($< 10^{-8}$);
- High trigger efficiency ($> 95\%$);

Table 2. Rates on principal detectors.

Detector	**Rate (MHz)**
CEDAR	50
GTK	800
LAV	9.5
STRAWS	8
RICH	8.6
LKR	10.5
MUV	9.2
SAC	1.5
Muon Halo	1

- Fully monitored systems;
- Readout without zero suppression for candidates;
- Low random veto probability at trigger level;
- Scalability in terms of bandwidth.

The first request is uncommon in other DAQ systems, but it's crucial for the NA62 experiment, where the full reconstruction of the background is an important issue. For the same reason zero suppression, mainly in the veto detectors, must be avoided as much as possible during the acquisition process. A good trigger efficiency can be obtained using information coming from several detectors with an excellent time resolution, in order to reduce the random veto probability.

A fully digital and integrated DAQ and trigger system has been designed: the digitization in the early stage of the readout system allows efficient monitoring of each stage of the chain, in order to detect any possible source of losses. The trigger system will be split into different levels: the first stage (L0), implemented in hardware using FPGAs, will be used to reduce the total rate to $\sim$ 1 MHz, while the second and third stages (L1 and L2) will be completely software based exploiting powerful PC-farms with large input bandwidth. The data accepted by the L2 will be directly transmitted to the CERN computer center, to be permanently recorded. The factor $\sim$ 10 in rate reduction at the first stage, will be obtained by a L0 trigger processor (L0TP) using information coming from RICH, LAV, LKr calorimeter and MUV detectors. The trigger primitives from each detector involved in the L0 trigger decision, will be built directly in the same data acquisition board devoted to digitization and monitoring: the TEL62 mother board, developed starting from the TELL1 board designed for the LHCb experiment [12]. The TEL62 board (9U format) houses 5 Altera Stratix III FPGAs allowing a fully customizable configuration. A total RAM memory of 8 GB gives the possibility to store the data in a first buffer stage, waiting for the trigger decision delivered to the board through the TTC [13] interface. A credit card PC (CCPC) allows to control all the functionality of the board. The output stage uses a quad GigaBit Ethernet card (total output bandwidth of 4 GB/s). The input stage can be adapted to different purposes using 4 custom daughter boards. For instance, the time of the data coming from the detectors front end could be digitized using the appositely developed TDCB daughter board[14]. The use of uniform system for all the subdetectors allows

to have a common fully integrated trigger and readout architecture, exploiting the possibility to use the same data chain to monitor the whole system and avoiding the complications due to independent trigger and readout chains. The L1 and L2 are completely in software. In the former the primitives are constructed using "single detector" information, while in the L2 the decision is taken on the information coming from all the detectors. Thanks to the trigger system the final acquisition rate will be of the order of tens of kHz.

A pilot project in the NA62 TDAQ, aims at investigating the use of the video card processors (GPU) for trigger purposes. The advantage of this approach is given by the huge computing power offered by the modern commercial GPUs at very competitive costs. The use of the video cards at L0, where the input rate is 10 MHz and the maximum latency is 1 ms, is very challenging, but is very promising to produce high quality primitives to build selective trigger conditions [15].

7. Conclusions

The ultra-rare $K^+ \to \pi^+\nu\bar{\nu}$ is an unique instrument to test the SM and to study possible contribution of new physics, thanks to clearness of the theoretical predictions. The possibility to distinguish between new physics model and to measure the dynamic structure of the coupling of the new physics particles, is complementary to the possible discover at hadron colliders. From an experimental point of view the measurement of this decay is very challenging due to the weakness of the signal signature and the presence of very huge background. The NA62 experiment aims at measuring O(100) events with 10% error. After three years of successful R&D program, the NA62 detector is now under construction and will be ready for commissioning and early physics runs in 2012.

References

[1] G. Buchalla and A. J. Buras, Nucl. Phys. B **548** (1999) 309 [arXiv:hep-ph/9901288].
[2] A. J. Buras, M. Gorbahn, U. Haisch and U. Nierste, JHEP **0611** (2006) 002 [arXiv:hep-ph/0603079].
[3] J. Brod and M. Gorbahn, Phys. Rev. D **78** (2008) 034006 [arXiv:0805.4119 [hep-ph]].
[4] G. Isidori, F. Mescia and C. Smith, Nucl. Phys. B **718** (2005) 319 [arXiv:hep-ph/0503107].
[5] A. J. Buras, B. Duling, T. Feldmann, T. Heidsieck and C. Promberger, JHEP **1009** (2010) 104 [arXiv:1006.5356 [hep-ph]].
[6] M. Blanke, A. J. Buras, B. Duling, S. Recksiegel and C. Tarantino, Acta Phys. Polon. B **41** (2010) 657 [arXiv:0906.5454 [hep-ph]].
[7] M. Blanke, PoS E **PS-HEP2009** (2009) 196 [arXiv:0908.2716 [hep-ph]].
[8] W. Altmannshofer, A. J. Buras, S. Gori, P. Paradisi and D. M. Straub, Nucl. Phys. B **830** (2010) 17 [arXiv:0909.1333 [hep-ph]].
[9] A. V. Artamonov *et al.* [BNL-E949 Collaboration], Phys. Rev. D **79** (2009) 092004 [arXiv:0903.0030 [hep-ex]].
[10] A. Antonelli *et al.*, J. Phys. Conf. Ser. **160** (2009) 012020 [Nucl. Phys. Proc. Suppl. **197** (2009) 224].
[11] V. Fanti *et al.* [NA48 Collaboration], Nucl. Instrum. Meth. A **574** (2007) 433.
[12] G. Haefeli, A. Bay, A. Gong, H. Gong, M. Muecke, N. Neufeld and O. Schneider, Nucl. Instrum. Meth. A **560** (2006) 494.
[13] B. G. Taylor [RD12 Project Collaboration], IEEE Trans. Nucl. Sci. **45** (1998) 821.
[14] C. Avanzini *et al.* [NA62 Collaboration], Nucl. Instrum. Meth. A **623** (2010) 543.
[15] G. Collazuol, G. Lamanna, M. Sozzi Nucl. Instrum. Meth. A **628** (2011) 457.